

# COMPARATIVE STUDY OF MAGNETIC PROPERTIES FOR CERN BEAM CURRENT TRANSFORMERS

S. Aguilera<sup>1,\*</sup>, H. Hofmann<sup>1</sup>, P. Odier  
CERN, Geneva, Switzerland

<sup>1</sup>also at École Polytechnique Fédérale de Lausanne, Lausanne, Switzerland

## Abstract

At CERN, the circulating beam current measurement is provided by two types of transformer, the Direct Current Current Transformer and the Fast Beam Current Transformer. Each transformer is built based on toroidal cores made from a soft magnetic material. Depending on the type of measurement to be performed these cores require different magnetic characteristics for parameters such as permeability, coercivity and the shape of the magnetisation curve. In order to study the effect of changes in these parameters on the current transformers, several interesting raw materials based on their as-cast properties were selected. The materials have been characterised to determine their crystallisation, melting and Curie Temperatures in order to determine suitable annealing processes to tailor their properties. They have been analysed by several techniques including Electron Microscopy and X-ray Diffraction. As-cast magnetic properties such as the permeability, the B-H curve and Barkhausen noise have also been measured to enable the study of the effect of thermal treatment in the microstructure of the alloys, and the correlation of this with the change in the magnetic properties.

## INTRODUCTION

The total electrical charge of the beam circulating in CERN's accelerators is measured by a family of devices that include current transformers, such as the DC Current Transformers (DCCT) and Fast Beam Current Transformers (FBCT) [1]. This measurement is especially crucial for tuning the beam transfer efficiency between accelerators, monitoring beam losses leading to possible radiation-related issues, assessing beam lifetime, as well as for safety measures to be taken based on the readings. There are a total of 96 transformers at CERN out of which 22 are DCCTs and 74 are FBCTs, coming in various sizes in order to adapt to different vacuum chamber dimensions.

The transformer cores are made out of wound ribbons of soft magnetic material which couple to the electro-magnetic fields accompanying the motion of the charged particle beams. Each type of transformer requires different magnetic materials in terms of permeability, coercivity and the shape of the magnetisation curve to obtain an optimal response for the differing beam parameters of each machine. The choice of material and the associated magnetic characteristics affects transformer parameters such as resolution in the case of the DCCT and bandwidth in case of the FBCT.

The study of commercially available soft magnetic materials, including physical properties such as crystallisation and melting temperatures, and magnetic properties like their Curie temperature and the magnetisation curve, will determine their suitability for each kind of instrument. With this information, a suitable annealing procedure can then be designed for each material. Thermal or thermo-magnetic annealing can drastically change the magnetic properties of the raw materials. The time and heating rate of annealing are the two key parameters that play a crucial role in the final result, enabling for example, the fabrication of nanocrystalline material. By being able to fabricate different cores, it is possible to study how these properties affect the final beam response of such systems in order to find the best solution for each type of application.

## MATERIALS USED

For this study, the materials used were iron-based amorphous and nanocrystalline alloys and cobalt-based amorphous alloys. Two iron-based alloys were purchased from Qinhuangdao Yanqin Nano Science & Technology Co., Ltd., Nanocrystalline 107A1 and amorphous 2065, with the Iron-based amorphous alloy FINEMET<sup>®</sup> FT-3 bought from Hitachi Metals Europe GmbH. The amorphous cobalt-based materials were purchased from Nanostructured & Amorphous Materials (Nanoamor), Inc., VACUUMSCHMELZE GmbH & Co. KG as VAC 6025 G40 Z and alloy Metglas 2705M from Hitachi Metals. Several cores made out of iron-based nanocrystalline material NANOPERM<sup>®</sup> were also bought from MAGNETEC GmbH, to be used as a reference material in the study.

## MATERIAL CHARACTERISATION

In order to thermally anneal the samples properly and understand the changes in their magnetic properties, it is first necessary to thoroughly characterise the alloys. Magnetic measurements like permeability, B-H curve and Barkhausen Noise will give an indication of the final performance of the material when in use in the instrument. Repeating these measurements after the annealing process then allows us to understand how the magnetic properties change during the treatment. The main goal being to tune the final magnetic properties through annealing.

### *Permeability and B-H Curve Measurements*

The relative complex permeability was calculated from the impedance measured with the Agilent Vector Impedance Analyser 4294 in the range of 40 Hz to 110 MHz. Cores of

\* silvia.aguilera@cern.ch

40 mm external diameter were used. The real and imaginary parts of permeability were derived from the in-series inductance and resistance of the core (following reference [2]) and uncertainty was calculated following [3]. The results are summarised in Table 1, where it can be seen that the iron-based materials (Yanqin and Finemet) have a lower permeability than the cobalt-based materials. All results have an uncertainty below 10 %.

Table 1: Maximum Relative Complex Permeability ( $\mu_R$ ) summary.

Sample	$\mu_R$
Yanqin amorphous	1171
Yanqin nanocrystalline	697
Finemet FT-3	1219
VAC 6025 G40	165626
Nanoamor	158110
Metglas 2705M	250802

B-H curve measurements were performed at a frequency of 212 Hz on the same cores. Table 2 shows a summary of the coercivity and saturation derived from these measurements, where it can be seen that the cobalt-based alloys present a lower coercivity than the iron-based alloys.

Table 2: Coercivity ( $H_C$ ) [ $A\ m^{-1}$ ] and Saturation ( $B_{sat}$ ) [T] for all Samples.

Sample	$H_C$ [ $A\ m^{-1}$ ]	$B_{sat}$ [T]
Yanqin amorphous	14.98	0.27
Yanqin nanocrystalline	19.43	0.62
Finemet FT-3	14.37	0.18
VAC 6025 G40	7.62	0.50
Nanoamor	4.47	0.45
Metglas 2705M	9.63	0.59

### Curie Temperature

The Curie temperature ( $T_C$ ) is a key parameter for the annealing process. Above this, the material loses its magnetic properties. This makes the rearrangement of magnetic domains possible during the thermal treatment, which can therefore mean a change in the magnetic properties of the sample. Annealing over  $T_C$ , but below the crystallisation point also allows the sample to relax internal stresses generated during the fabrication process without changing the microstructure.

The Curie temperature was measured with a Thermo gravimetric Analysis Instrument (PerkinElmer TGA 4000) in a magnetic field. The PerkinElmer 4000 has an oven temperature uncertainty of 1.8 °C, and a sample temperature uncertainty of  $\pm 0.8$  °C at 300 °C and  $\pm 1.5$  °C at 900 °C. The balance uncertainty is  $\pm 0.03$  % [4]. The total uncertainty for the measurement is  $\pm 2.6$  °C. Table 3 shows the results for the heating curve at 10 °C  $min^{-1}$ .

Table 3: Curie Temperature ( $T_C$ ) at 10 °C  $min^{-1}$ . Uncertainty for all measurements is  $\pm 2.6$  °C

Sample	$T_C$ [°C]
Yanqin amorphous	319
Yanqin nanocrystalline	405
Finemet FT-3	319
Magnetec	565
VAC 6025 G40	222
Nanoamor	223
Metglas 2705M	361

### Crystallisation and Melting Point Characterisation

Crystallisation and melting temperatures are characteristic of each alloy that change with composition. They are therefore not only essential input for the annealing process, but also as a means to compare various alloys. The crystallisation temperature becomes the key parameter when the amorphous samples are to be transformed into nanocrystalline materials.

These measurements were performed with alumina pans in a Netzsch DSC 404 C under an argon atmosphere at 10 °C  $min^{-1}$ . All the curves were started from room temperature, as will be the case when the material are annealed in an oven. Table 4 summarises the onset and peak crystallisation temperatures found.

Table 4: Onset Crystallisation Temperature ( $T_O$ ), Peak Crystallisation Temperature ( $T_P$ ) and Area of the Curve (A) at 10 °C  $min^{-1}$ .

Sample	$T_O$ [°C]	$T_P$ [°C]	A [ $J\ g^{-1}$ ]
Yanqin amor.	507.8	529.5	63.4
	686.0	700.0	19.3
Yanqin nano.	498.1	507.7	43.1
	540.3	544.8	67.7
Finemet FT-3	507.5	527.4	61.8
	695.1	703.8	26.2
Magnetec	681.4	693.3	16.4
	718.1	730.0	3.3
VAC 6025 G40	546.3	552.3	65.2
	613.1	638.4	33.7
Nanoamor	548.2	549.1	73.6
	597.4	626.4	7.9
Metglas 2705M	511.6	529.1	-
	-	554.2	72.3
	638.2	656.2	30.2

The onset melting temperatures ( $T_M$ ) and their standard deviation ( $\sigma$ ) are summarised in Table 5. It can be seen that the cobalt-based alloys have a melting temperature of about 100 °C lower than the iron-based alloys.

Table 5: Melting Temperatures

Sample	$T_M$ [°C]	$\sigma$ [°C]
Yanqin amor.	1102.4	0.2
Yanqin nano.	1139.1	0.5
Finemet FT-3	1102.6	0.5
Magnetec	1104.2	0.0
VAC 6025 G40	1011.7	1.0
Nanoamor	1007.6	1.4
Metglas 2705M	1007.1	2.6

### X-ray Diffraction (XRD) Analyses

The XRD studies are a useful tool to check for the presence of ordered regions (crystals) in the samples. Changes in the microstructure of the alloy, being amorphous, nanocrystalline or completely crystalline, entirely changes its magnetic and mechanical properties. It is therefore important to know what state the material is in in its as-cast state and how it evolves under thermal treatment. A High-Energy XRD study will show the microstructure of the as-cast sample, while a High-Temperature in-situ XRD (HT-XRD) allows the evolution of the sample during thermal treatment to be studied.

For the High-Energy XRD the samples were analysed by Phase Solutions Co. Ltd. at the ESRF (European Synchrotron Radiation Facility), after pulverisation. The diffraction images were recorded at room temperature using an incident X-ray beam with a cross-section of 3 mm by 3 mm.

It can be seen from Table 6 that all of the samples present a certain degree of crystallinity. Only the Magnetec sample can be considered nanocrystalline (with crystals larger than 5 nm), as it has an average crystal size of 14.3 nm.

Table 6: Average Crystal Size and Standard Deviation ( $\sigma$ ) Measured by HE-XRD

Sample	Average crystal size $\pm\sigma$ [nm]
Yanqin amorphous	$1.6 \pm 0.2$
Yanqin nanocrystalline	$1.5 \pm 0.2$
Finemet FT-3	$2.0 \pm 0.2$
Magnetec	$14.3 \pm 0.2$
VAC 6025 G40	$2.0 \pm 0.2$
Nanoamor	$2.2 \pm 0.2$
Metglas 2705M	$1.9 \pm 0.2$

The HT-XRD experiments were performed in the Swiss Center for Electronics and Microtechnology (CSEM) in Neuchâtel. Samples were heated at a rate of  $10^\circ\text{C min}^{-1}$  under a nitrogen atmosphere. Table 7 shows the crystallisation temperature results and the proposed crystalline composition of the samples studied up to now. The results are consistent both with the composition and the crystallisation temperature characterisation.

Table 7: Crystallisation Temperatures ( $T_X$ ) and Crystal Composition Detected by HT-XRD

Sample	$T_X$ [°C]	Crystal composition
Finemet FT-3	550 - 575	$\text{Co}_2\text{Si}$
Nanoamor	550 - 575	$\text{Co}_2\text{Si}, \text{Co}_{21}\text{Mo}_2\text{B}_6$
Metglas 2705M	550 - 575	$\text{Fe}_3\text{Si}$

### Transmission Electron Microscopy (TEM)

TEM was used in Bright-Field (BF) and Dark-Field (DF) mode. In the BF mode, the electrons from the microscope interact with the sample and give a darker projection where the sample is thicker or denser or where there are heavier atoms, so giving information on the composition. To obtain a DF image, the Diffraction Pattern (DP) of the sample is first obtained. Then, a point in the DP can be selected for observation and this gives the DF image. The bright areas will be the ones diffracting in that particular direction. DF images can give information on defects or particle sizes in the samples.

TEM measurements were taken with a TECNAI OSIRIS microscope and an 11 Megapixel Gatan Orius CCD camera. This TEM has 0.24 nm point resolution and a 0.14 nm information limit. Figure 1 shows the bright field of the Magnetec sample. It can be seen that there are crystals of about 20 nm in size, which is consistent with the XRD analyses. The rest of the samples show crystalline regions of much smaller size as measured by XRD.

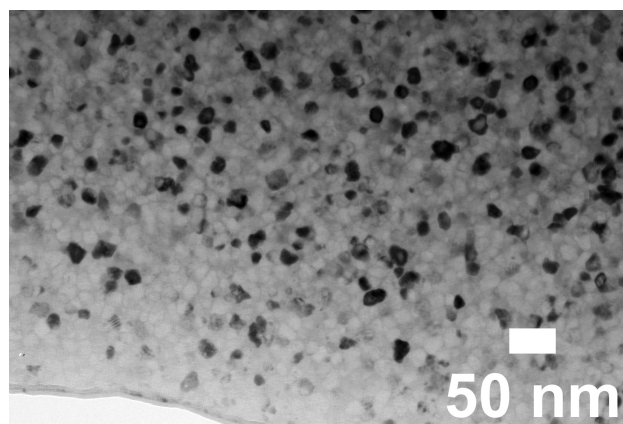


Figure 1: Bright-Field image of the Magnetec sample.

Figure 2 shows the DF image for the Magnetec sample and the DP in the insert. It can be seen that the diffracting crystals in this case are up to 25 nm in size, slightly bigger than the ones measured by XRD.

### Barkhausen Noise (BN) Measurements

Barkhausen noise measurements were performed using a setup based on that described in [5]. This was improved by additional common-mode chokes in order to limit the sensitivity of the setup to stray fields, and using a 30 mHz, 8 V peak-peak filtered triangular current for the driving solenoid.

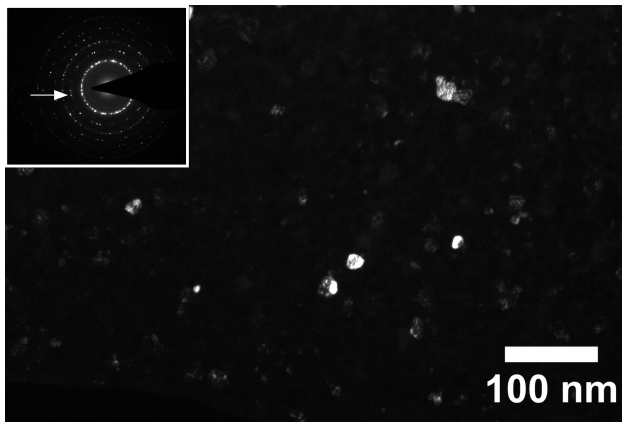


Figure 2: Dark-Field image of the Magnetec sample, the Diffraction Pattern can be seen in the insert.

50 averages were performed for each measurement. Figure 3 shows the BN measurement for Finemet (top) and the excitation signal (bottom). What can be seen is the voltage induced in the secondary coil surrounding the magnetic sample while it is subjected to the driving current. The voltage drops to zero when the sample is saturated.

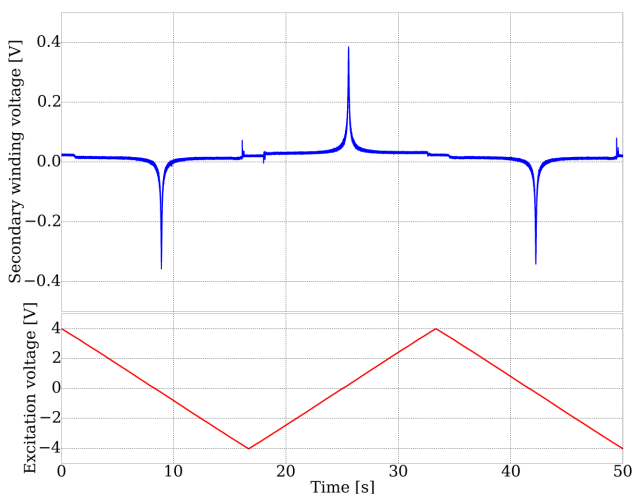


Figure 3: BN measurement for Finemet FT-3 (top) and excitation signal (bottom).

Figure 4 shows the BN (proportional to the secondary winding voltage) for VAC 6025. Once measured as-cast, the samples were annealed for half an hour above their  $T_C$  before being re-measured. As can be seen, the BN in this case decreases after annealing. A similar reduction in BN was found for Yanqin amorphous and Nanoamor, with Finemet showing an increase after annealing and Yanqin nanocrystalline and Metglas 2705M showing no significant change. Further XRD and magnetic domain visualisation studies of the annealed samples are being performed in order to understand these results, which may be caused by stress relaxation, dislocation displacement and crystal growth.

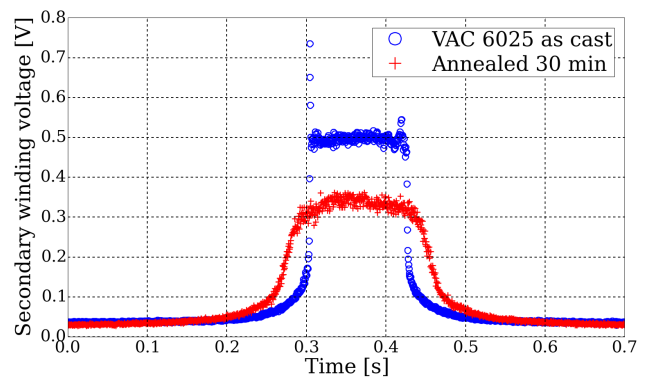


Figure 4: BN for VAC 6025 before and after annealing.

## CONCLUSIONS

Taking into account the measured magnetic properties of many different materials, it can be seen that there is a great difference between the iron-based and cobalt-based alloys. The latter present better as-cast properties in their amorphous state for use as transformer cores. However, the former could potentially be good materials in their nanocrystalline state, as nanocrystalline iron-based materials are known for their good magnetic properties and Finemet FT-3 is extensively used for building cores. Materials VAC 6025 and Nanoamor were found to have very similar properties and therefore only one needs to be maintained for further study. This leaves three materials to be studied in-depth for final exploitation as beam current transformer cores: Finemet FT-3, VAC 6025 and Metglas 2705M.

## ACKNOWLEDGMENTS

The authors would like to thank Michał Krupa, Jacques Longo, Dr. Emad Oveisi, Romain Ruffieux, Dr. Olha Sereda and Dr. Jérémy Tillier for their contribution to the results in this paper.

## REFERENCES

- [1] S. Aguilera, P. Odier and R. Ruffieux, "Magnetic Materials for Current Transformers", in Proc. International Beam Instrumentation Conference 2013 (IBIC2013), Oxford, UK, paper MOPF24, pp. 263-266, [Online], Available: <http://www.ibic2013.org/prepress/papers/mopf24.pdf>
- [2] Agilent Technologies, *Application Note 1369-1*, 2008, p. 17
- [3] "Agilent 4294A Precision Impedance Analyzer Operation Manual." Agilent Technologies Japan Ltd., Hyogo, Japan, 2003, p. 469.
- [4] "Technical Specifications for the TGA 4000 Thermogravimetric Analyzer", PerkinElmer Inc., 2009, [Online], Available: [http://www.perkinelmer.com/CMSResources/Images/46-74807SPC\\_TGA4000.pdf](http://www.perkinelmer.com/CMSResources/Images/46-74807SPC_TGA4000.pdf)
- [5] D. Spasojević, S. Bukvić, S. Milošević and H. Stanley, "Barkhausen noise: Elementary signals, power laws, and scaling relations", *Phys. Rev. E*, 3, Vol. 54, 1996, pp. 2531-2546.